

Rydberg electromagnetically induced transparency and Autler-Townes splitting in a weak radio-frequency electric field

Liping Hao(郝丽萍), Yongmei Xue(薛咏梅), Jiabei Fan(樊佳蓓), Yuechun Jiao(焦月春), Jianming Zhao(赵建明), Suotang Jia(贾锁堂)

Citation: Chin. Phys. B . 2019, 28(5): 053202. **doi:** 10.1088/1674-1056/28/5/053202
Journal homepage: http://cpb.iphy.ac.cn; http://iopscience.iop.org/cpb

What follows is a list of articles you may be interested in

Properties of collective Rabi oscillations with two Rydberg atoms

Dan-Dan Ma(马丹丹), Ke-Ye Zhang(张可烨), Jing Qian(钱静)
Chin. Phys. B . 2019, 28(1): 013202. **doi:** 10.1088/1674-1056/28/1/013202

Vapor cell geometry effect on Rydberg atom-based microwave electric field measurement

Linjie Zhang(张临杰), Jiasheng Liu(刘家晟), Yue Jia(贾玥), Hao Zhang(张好), Zhenfei Song(宋振飞), Suotang Jia(贾锁堂)
Chin. Phys. B . 2018, 27(3): 033201. **doi:** 10.1088/1674-1056/27/3/033201

Velocity-selective spectroscopy measurements of Rydberg fine structure states in a hot vapor cell

Jun He(何军), Dongliang Pei(裴栋梁), Jieying Wang(王杰英), Junmin Wang(王军民)
Chin. Phys. B . 2017, 26(11): 113202. **doi:** 10.1088/1674-1056/26/11/113202

Laser frequency locking based on Rydberg electromagnetically induced transparency

Yuechun Jiao(焦月春), Jingkui Li(李敬奎), Limei Wang(王丽梅), Hao Zhang(张好), Linjie Zhang(张临杰), Jianming Zhao(赵建明), Suotang Jia(贾锁堂)
Chin. Phys. B . 2016, 25(5): 053201. **doi:** 10.1088/1674-1056/25/5/053201

Lifetimes of Rydberg states of Eu atoms

Jing Hua, Ye Shi-Wei, Dai Chang-Jian
Chin. Phys. B . 2015, 24(1): 013203. **doi:** 10.1088/1674-1056/24/1/013203

Rydberg electromagnetically induced transparency and Autler–Townes splitting in a weak radio-frequency electric field*

Liping Hao(郝丽萍)[1], Yongmei Xue(薛咏梅)[1], Jiabei Fan(樊佳蓓)[1], Yuechun Jiao(焦月春)[1,2], Jianming Zhao(赵建明)[1,2,†], and Suotang Jia(贾锁堂)[1,2]

[1] *State Key Laboratory of Quantum Optics and Quantum Optics Devices, Institute of Laser Spectroscopy, Shanxi University, Taiyuan* 030006, *China*
[2] *Collaborative Innovation Center of Extreme Optics, Shanxi University, Taiyuan* 030006, *China*

(Received 11 January 2019; revised manuscript received 9 March 2019; published online 8 April 2019)

We utilize an electromagnetically induced transparency (EIT) of a three-level cascade system involving Rydberg state in a room-temperature cell, formed with a cesium $6S_{1/2}$–$6P_{3/2}$–$66S_{1/2}$ scheme, to investigate the Autler–Townes (AT) splitting resulting from a 15.21-GHz radio-frequency (RF) field that couples the $|66S_{1/2}\rangle \rightarrow |65P_{1/2}\rangle$ Rydberg transition. The radio-frequency electric field induced AT splitting, $\gamma_{\rm AT}$, is defined as the peak-to-peak distance of an EIT-AT spectrum. The dependence of AT splitting $\gamma_{\rm AT}$ on the probe and coupling Rabi frequency, $\Omega_{\rm p}$ and $\Omega_{\rm c}$, is investigated. It is found that the EIT-AT splitting strongly depends on the EIT linewidth that is related to the probe and coupling Rabi frequency in a weak RF-field regime. Using a narrow linewidth EIT spectrum would decrease the uncertainty of the RF field measurements. This work provides new experimental evidence for the theoretical framework in [*J. Appl. Phys.* **121**, 233106 (2017)].

Keywords: Rydberg electromagnetically induced transparency-Autler–Townes (EIT-AT), cascade four-level atom, radio-frequency (RF) electric field

PACS: 32.80.Ee, 42.50.Gy, 71.70.–d, 84.40.–x **DOI:** 10.1088/1674-1056/28/5/053202

1. Introduction

In recent decades, atom-based metrology has had a tremendous impact on science, technology, and human life, such as optical atomic clocks[1,2] and the global positioning system, and highly sensitive position-resolved magnetometers.[3,4] Atom-based field measurement has clear advantages over other field measurement methods, due to their invariable level structure that can be used as a calibration-free criterion. Rydberg atom, a highly excited atom with principal quantum number $n > 10$, has a large electric polarizability, scaling $\propto n^7$, and big microwave-transition dipole moments, scaling $\propto n^2$.[5] These properties make Rydberg atoms good candidates for measuring an external electric field.[6–14] The electromagnetically induced transparency (EIT)[15] involving Rydberg states that provides a non-destructive optical detection of Rydberg states[16] has been widely investigated in recent years. Rydberg EIT is employed to measure the electric field of electromagnetic radiation with a large dynamic range,[6] demonstrating a number of applications, such as measurements of microwave fields,[6–10] millimeter waves,[11] static electric fields,[12–14] sub-wavelength imaging of microwave electric field distributions,[17,18] field inhomogeneities,[19] and back scattered electric field of identification tag.[20]

The radio-frequency (RF) electric field with a frequency greater than 1 GHz has been measured based on an Autler–Townes (AT) effect[21] where the RF field couples the nearby Rydberg levels.[7] The AT splitting is known as an AC Stark effect. The AT splitting $\gamma_{\rm AT}$, defined as the peak-to-peak distance of AT spectrum, is proportional to the amplitude of RF-field $E_{\rm RF}$, i.e., $\gamma_{\rm AT} = \Omega_{\rm RF} = \mu_{\rm RF}E_{\rm RF}/\hbar$, where $\Omega_{\rm RF}$ is the RF-field Rabi frequency, $\mu_{\rm RF}$ is the RF-field coupled dipole matrix element, and $\hbar$ is the reduced Planck constant. Rydberg EIT is employed to measure the AT splitting, and further the RF electric field. The Rydberg EIT-AT spectrum yields a direct International System of Units (SI) traceable, self-calibrated, and broad band measurement of microwave electric field, which has the capability to realize measurements on a fine spatial resolution. The approach of EIT/AT-based electric-field measurement has recently been investigated by several groups around the world.[6–9,11]

Rydberg EIT is employed to measure the RF-field induced AT splitting. The EIT linewidth would strongly affect the accuracy of field measurements, which was discussed theoretically in Ref. [9]. In this work, we provide experimental evidence that agrees with the theoretical calculation of Ref. [9]. We present Rydberg EIT-AT spectra in a cesium room-temperature vapor cell, where a 15.21-GHz RF field couples the $|66S_{1/2}\rangle \rightarrow |65P_{1/2}\rangle$ Rydberg transition for producing the AT splitting $\gamma_{\rm AT}$. We investigate the dependence of $\gamma_{\rm AT}$ on EIT linewidth by varying the coupling and probe laser Rabi frequency. The residuals are used to describe the devi-

*Project supported by the National Key Research and Development Program of China (Grant No. 2017YFA0304203), the National Natural Science Foundation of China (Grant Nos. 61475090, 61675123, 61775124, and 11804202), the State Key Program of National Natural Science of China (Grant Nos. 11434007 and 61835007), and the Changjiang Scholars and Innovative Research Team in University of Ministry of Education of China (Grant No. IRT13076).

†Corresponding author. E-mail: zhaojm@sxu.edu.cn

© 2019 Chinese Physical Society and IOP Publishing Ltd

ations between calculations and measurements of the EIT-AT spectra. It is found that the smaller coupling and probe laser Rabi frequencies can decrease the uncertainty of the RF electric field measurements in a weak RF-field regime.

2. Experimental setup

We perform Rydberg EIT-AT experiments in a vapor cell, and the experimental setup and a relevant four-level Rydberg-EIT-AT scheme are shown in Figs. 1(a) and 1(b). A weak probe laser at a wavelength of $\lambda_p = 852$ nm is produced by an external cavity diode laser (Toptica DLpro), and a strong coupling laser at a wavelength of $\lambda_c = 510$ nm is produced with a commercial laser (Toptica SHG110). The probe and coupling lasers overlap and counter-propagate through a room-temperature cylindrical cesium vapor cell with a length of 25 mm and a diameter of 25 mm. The probe frequency is stabilized to the $|6S_{1/2}\ F=4\rangle \rightarrow |6P_{3/2}\ F'=5\rangle$ transition using a polarization spectrum technique, while the coupling laser frequency is ramped over the $|6P_{3/2}\ F'=5\rangle \rightarrow |66S_{1/2}\rangle$ Rydberg transition. The EIT spectrum is detected by measuring the transmission of the probe laser using a photodiode (PD) after a dichroic mirror (DM).

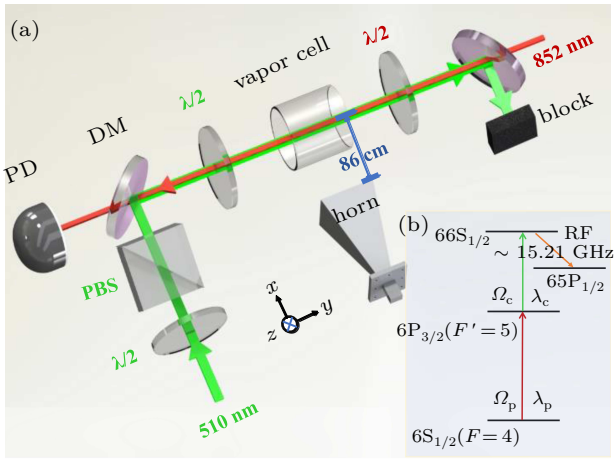


Fig. 1. (a) Schematic diagram of the experiment. The coupling ($\lambda_c = 510$ nm) and probe ($\lambda_p = 852$ nm) beams counter-propagate through a cesium vapor cell along the y-axis. The horn placed 86 cm from the cell (not scaled) emits an RF electric field with a frequency ~ 15.21 GHz for coupling the Rydberg transition and producing an EIT-AT spectrum. The horn is set such that the RF electric field is linearly polarized along the z-axis which is parallel to the polarizations of the probe and coupling laser beams. The probe beam passing through a cesium cell and a dichroic mirror is detected with a photodiode. The PBS indicates polarization beam splitter. (b) The energy level diagram of the cesium four-level system. The probe laser λ_p is resonant with the $|6S_{1/2}\ F=4\rangle \rightarrow |6P_{3/2}\ F'=5\rangle$ lower transition, and the coupling laser λ_c is scanned through the $|6P_{3/2}\ F'=5\rangle \rightarrow |66S_{1/2}\rangle$ Rydberg transitions. The applied RF electric field couples the transition $|66S_{1/2}\rangle \rightarrow |65P_{1/2}\rangle$, yielding a Rydberg EIT-AT spectrum.

The probe and coupling beams have Gaussian waist $\omega_{0p} = 90$ μm and $\omega_{0c} = 135$ μm in the cell, respectively. The corresponding Rabi frequency can be calculated with the formula $\Omega_{p(c)} = \frac{\mu_{p(c)}}{\hbar}\sqrt{\frac{2P_{p(c)}}{\pi\omega_{0p(c)}^2 c\varepsilon_0}}$, where $P_{p(c)}$ is the probe (coupling) laser power, $\omega_{0p(c)}$ is a beam waist, ε_0 is the permittivity in vacuum, and c is the speed of light. The $\mu_{p(c)}$ indicates the transition dipole moment of the probe (coupling) coupled transition. Both the coupling and probe laser Rabi frequencies affect the EIT linewidth γ_{EIT}. Here, we vary the probe/coupling laser power to change the Rabi frequency with a series of neutral attenuators.

A 15.21-GHz RF electric field, produced with a function generator (Agilent N5183B) and emitted by a horn antenna, is applied transversely to the laser beam through the cell, where the RF field couples the Rydberg transition $|66S_{1/2}\rangle \rightarrow |65P_{1/2}\rangle$ and yields splitting of the EIT spectrum, e.g., Rydberg EIT-AT spectrum. The calculated radical dipole moment μ_{RF} is 3942 ea_0. The AT splitting γ_{AT} is defined as the peak-to-peak distance of EIT-AT spectrum, which is used to measure the RF electric field. The RF electric field is linearly polarized along the z-axis, parallel to the polarization of the probe and coupling lasers. This configuration yields the two-peak EIT-AT spectral profile. The RF electric field is expressed as $E_{RF} = \sqrt{30P_{RF}g}/d$,[22] where P_{RF} is the power of the microwave source, g is a gain of the antenna, and d is a distance from the antenna to the cell. The calculated far-field condition d_0 is about 65 cm in this work, and the horn antenna is set to 86-cm away from the cell, which is larger than the far-field condition d_0. The experimental region is surrounded by the microwave-absorbing material to avoid unwanted reflections.

3. Results and discussion

Rydberg EIT is a quantum interference process in which the absorption of a weak probe laser, interacting resonantly with an atomic transition, is reduced in the presence of a coupling laser, which (near-) resonantly couples the upper probe level to a Rydberg state.[16] Rydberg EIT is employed to perform an optical detection of Rydberg level and AT splitting induced by an RF electric field that is coupled to the nearby Rydberg states.

In Fig. 2(a), we present Rydberg EIT-AT spectra with an up level $|66S_{1/2}\rangle$ Rydberg state and a 15.21-GHz microwave electric field coupling $|66S_{1/2}\rangle \rightarrow |65P_{1/2}\rangle$ transition. The probe and coupling beam Rabi frequencies are $\Omega_p = 2\pi \times 3.99$ MHz and $\Omega_c = 2\pi \times 2.06$ MHz, respectively. We obtain an EIT peak at two-photon detuning $\delta = 0$, as shown by the black symbols in Fig. 2(a). The EIT linewidth $\gamma_{EIT} = 2\pi \times 4.68$ MHz, extracted by a Lorentz fitting to the experimental data, is close to the natural linewidth $\Gamma_{eg} = 2\pi \times 5.2$ MHz of the intermediate state. The EIT spectrum is calibrated by the hyperfine level $|6P_{3/2}\ F'=4\rangle$ Rydberg EIT signal, which is not shown here; see Ref. [12] for more details. When we apply an RF electric field that drives the $|66S_{1/2}\rangle \rightarrow |65P_{1/2}\rangle$ Rydberg transition, the EIT line peak decreases and separates

into two peaks as the RF field increases, known as the AT splitting γ_{AT}. The AT splitting γ_{AT} is defined as the peak-to-peak distance of EIT-AT spectrum and extracted using the multi-peak Lorentz fittings to the data. Figure 2(a) displays EIT-AT spectra with two indicated RF powers. The measured γ_{AT} values are $2\pi \times 9.48$ MHz and $2\pi \times 24.96$ MHz for microwave power of 0.32 mW and 1.99 mW, respectively. The γ_{AT} shows a linear increase with a square root of RF power, amplitude of the RF field, which is the chief gauge for measuring RF electric field based on the Rydberg atom.

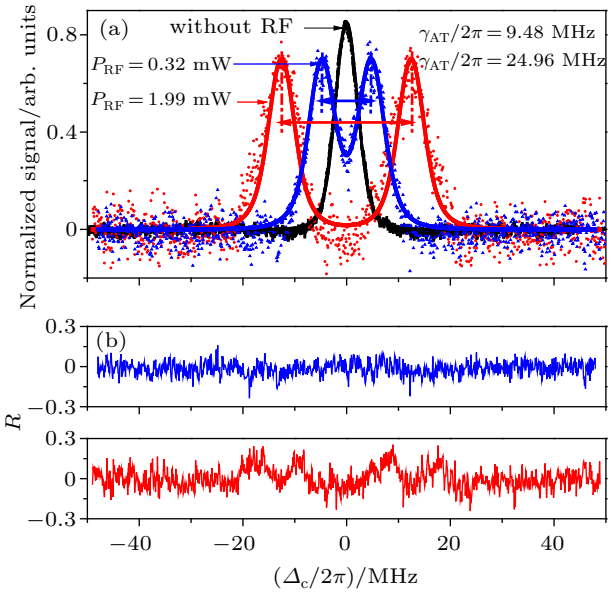


Fig. 2. (a) Measurements (symbols) and calculations (solid lines) of Rydberg EIT-AT spectra as a function of the coupling laser detuning Δ_c for fixed probe/coupling laser Rabi frequency $\Omega_p = 2\pi \times 3.99$ MHz and $\Omega_c = 2\pi \times 2.06$ MHz and an indicated microwave power $P_{RF} = 0.32$ mW (blue) and 1.99 mW (red). The RF electric field with frequency 15.21 GHz couples the nearby Rydberg states $|66S_{1/2}\rangle$ and $|65P_{1/2}\rangle$. The AT splitting γ_{AT} is obtained by multipeak Lorentz fittings to the Rydberg EIT-AT spectra. The RF field-free EIT signal (black) is obtained with a $6S_{1/2}$–$6P_{3/2}$–$66S_{1/2}$ three-level scheme, and a Lorentz fitting to the data yields an EIT linewidth $\gamma_{EIT} = 2\pi \times 4.68$ MHz. (b) The residuals R between experiment and theory. The RMS values of the residuals are 0.052 and 0.079 for $P_{RF} = 0.32$ mW and 1.99 mW, respectively, showing good agreement with the experimental data. The small fluctuations near the center of the line are attributed to the broadening that is mainly induced by the inhomogeneity of the RF field, see text.

For comparison with the theory, we simulate the EIT-AT spectrum by numerically solving the master equation

$$\dot{\rho} = -\frac{i}{\hbar}[H, \rho] + \mathfrak{L}, \tag{1}$$

where H is the Hamiltonian of the four-level atomic system in Fig. 1(b), and $\mathfrak{L}$ is the Lindblad operator that accounts for the decay processes of the atom. The details of the decay term, $\mathfrak{L}$, are described in our previous work[23] and Ref. [9]. The simulations of EIT-AT spectra are displayed with solid lines in Fig. 2(a). In Fig. 2(b), we present the residuals between experiment and theory for further comparison, and the corresponding root mean square (RMS) values of residuals are respectively 0.052 and 0.079 for RF power $P_{RF} = 0.32$ mW and 1.99 mW, showing good agreement. There are some small but noticeable structures for the case of $P_{RF} = 1.99$ mW near the center of the line, which is attributed to the line broadening caused by the inhomogeneity of the RF field. Atoms interacting with the laser field experience different fields due to the inhomogeneity of the RF field in the cesium cell, leading to the broadened line and even multi-peak EIT-AT spectra.[22]

For a weak RF electric field, it is noted that the measured AT splitting γ_{AT} strongly depends on the EIT linewidth γ_{EIT} that is relevant to the coupling and probe laser Rabi frequency. To investigate the dependence of EIT-AT splitting γ_{AT} on the EIT linewidth, we keep the RF Rabi frequency Ω_{RF} fixed and vary the Rabi frequency of probe/coupling laser to do a series of γ_{AT} measurements. As an example, in Fig. 3(a), we plot γ_{AT} as a function of Ω_p while keeping $\Omega_c = 2\pi \times 2.06$ MHz and $\Omega_{RF} = 2\pi \times 7.61$ MHz (corresponding to $E_{RF} = 0.46$ V/m) fixed. The measured $\gamma_{AT} \approx \Omega_{RF}$ at small Ω_p and shows a decrease with Ω_p. The dependence of γ_{AT} on Ω_c is also plotted in Fig. 3(b), and γ_{AT} again displays a decrease with Ω_c. We attribute this $\Omega_{p(c)}$ dependence of γ_{AT} in Fig. 3 to the Rydberg EIT linewidth γ_{EIT}, which is used to measure the RF-induced AT splitting. In a weak field regime, when $\gamma_{EIT} > \Omega_{RF}$, RF induced AT splitting cannot be distinguished at all, whereas as $\gamma_{EIT} \simeq \Omega_{RF}$, AT splitting is distinguishable but measured γ_{AT} would depend on the EIT linewidth. For the case here, $\Omega_c, \Omega_p \lesssim \Gamma_{eg}$, the EIT linewidth is expressed as

$$\gamma_{EIT} = (\Omega_c^2 + \Omega_p^2)/\Gamma_{eg}. \tag{2}$$

RF-free EIT γ_{EIT} depends on Ω_c and Ω_p. The other possible reason leading to $\gamma_{AT} < \Omega_{RF}$ is AT splitting being the nonlinear dependence regime, an intrinsic behavior of EIT or AT spectrum, which is beyond the scope of this work. See Ref. [9] for details.

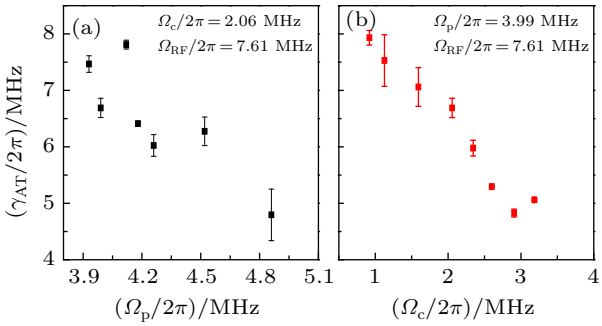


Fig. 3. (a) Measurements of γ_{AT} as a function of the probe Rabi frequency Ω_p for fixed $\Omega_c = 2\pi \times 2.06$ MHz and $\Omega_{RF} = 2\pi \times 7.61$ MHz. (b) Similar measurements analogous to (a) as a function of the coupling Rabi frequency Ω_c for fixed $\Omega_p = 2\pi \times 3.99$ MHz.

In order to investigate how the probe/coupling laser Rabi frequency affects the AT splitting γ_{AT} and further the RF electric field measurement, we demonstrate EIT-AT spectra (symbols) and simulations (solid line) with a fixed RF field and

two different probe laser Rabi frequencies in Fig. 4 to analyze the uncertainty in the field-measurements. The RF Rabi frequency is set to be $\Omega_{\rm RF} = 2\pi \times 7.73$ MHz, corresponding to the electric field amplitude of 0.47 V/m. For the smaller $\Omega_{\rm p} = 2\pi \times 3.93$ MHz in Fig. 4(a), the EIT-AT spectrum has two peaks that separate well, and the multipeak Lorentz fitting yields AT splitting $\gamma_{\rm AT} = 2\pi \times 7.86$ MHz, which is closer to the $\Omega_{\rm RF}$. We define the deviation $D_{\rm Err} = (\gamma_{\rm AT} - \Omega_{\rm RF})/\Omega_{\rm RF}$ to describe the relative error of RF field measurement, and $D_{\rm Err} = 1.68\%$ in Fig. 4(a). For the larger $\Omega_{\rm p} = 2\pi \times 4.51$ MHz in Fig. 4(b), two peaks in EIT-AT spectrum are just distinguishable, measured $\gamma_{\rm AT} = 2\pi \times 6.27$ MHz is -18.89% that is less than the expectation. We attribute this to an increased probe laser $\Omega_{\rm p}$ that results in the broadened EIT linewidth. When the EIT linewidth approaches the AT splitting, the two peaks of EIT-AT spectrum become indistinguishable, see Fig. 4(b). The EIT-AT spectrum even turns into one peak when $\gamma_{\rm EIT}$ is larger than $\gamma_{\rm AT}$. In the weak field regime, the EIT-AT splitting $\gamma_{\rm AT}$ decreases with $\Omega_{\rm p}$, which causes big uncertainty $D_{\rm Err}$.

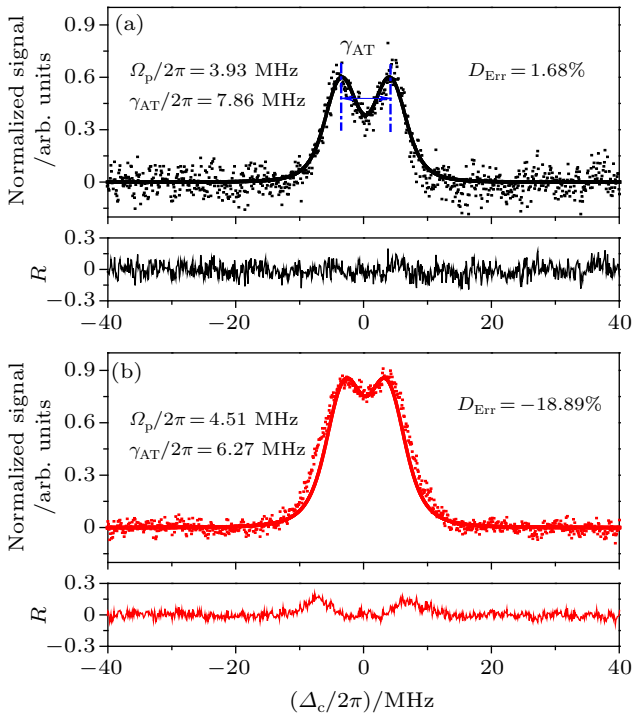


Fig. 4. Measurements (symbols) and calculations (solid lines) of Rydberg EIT-AT spectra as a function of the coupling laser detuning $\Delta_{\rm c}$ for fixed $\Omega_{\rm c} = 2\pi \times 2.06$ MHz and $\Omega_{\rm RF} = 2\pi \times 7.73$ MHz at two different probe Rabi frequencies (a) $\Omega_{\rm p}/2\pi = 3.93$ MHz and (b) 4.51 MHz. The deviation $D_{\rm Err}$ is obtained with the ratio $(\gamma_{\rm AT} - \Omega_{\rm RF})/\Omega_{\rm RF}$. The bottom panel shows the residuals R between the measured and calculated EIT-AT spectra, and the RMS values of residuals are (a) 0.063 and (b) 0.050.

Closely inspecting Fig. 4, we find that the signal-to-noise ratio of the EIT-AT spectrum for small $\Omega_{\rm p}$ in Fig. 4(a) is less than that for large $\Omega_{\rm p}$ in Fig. 4(b). This is because the small probe laser power results in a large background noise. At the bottom of Fig. 4, we plot the residuals between the measurements and calculations of the EIT-AT spectra. The RMS values of the residuals are 0.063 and 0.050 for $\Omega_{\rm p}/2\pi = 3.93$ MHz (Fig. 4(a)) and 4.51 MHz (Fig. 4(b)), respectively. Figure 4 demonstrates that the narrow EIT linewidth using the small probe Rabi frequency could increase the accuracy of a weak RF-field measurement. However, further decrease of the probe $\Omega_{\rm p}$ will lead to large background noise, see Fig. 4(a), which may also yield large measurement uncertainty. Furthermore, we also do the test of the coupling Rabi frequency as Fig. 4 and obtain similar results, as the coupling Rabi frequency broadens the EIT linewidth as demonstrated in Eq. (2). In experiments, we need to balance the EIT linewidth and spectrum sensitivity in the RF-field measurements.

4. Conclusion

In conclusion, we have investigated Rydberg EIT-AT spectra employing a cesium ladder four-level system involving Rydberg $|66S_{1/2}\rangle$, in which a 15.21-GHz RF field couples the nearby Rydberg states transition $|66S_{1/2}\rangle \rightarrow |65P_{1/2}\rangle$. An RF field results in the AT splitting of the EIT resonance $\gamma_{\rm AT}$ which is proportional to the RF-coupled Rabi frequency $\Omega_{\rm RF} = \mu_{\rm RF} E_{\rm RF}/\hbar$, providing a calibration-free and broad band measurement of RF electric field.[7] However, in a weak RF field regime, the AT splitting strongly depends on the RF-free EIT linewidth that is related to the coupling/probe laser Rabi frequency. It is found that the measured AT splitting $\gamma_{\rm AT}$ decreases with probe and coupling Rabi frequency $\Omega_{\rm p(c)}$. We have attributed this behavior to two causes. The first one is broadened Rydberg EIT linewidth due to the laser Rabi frequency. When the EIT linewidth is $\gamma_{\rm EIT} \gtrsim \Omega_{\rm RF}$, two peaks of EIT-AT spectrum become indistinguishable that leads to smaller $\gamma_{\rm AT}$. The experimental results are analyzed by the four-level model of Ref. [9]. The second one is the nonlinear dependence of the EIT-AT splitting on the RF field in the weak RF field regime. For RF electric field measurements, using narrow linewidth EIT would compress the nonlinear zoom of EIT-AT splitting and increase the field measurements accuracy, but it is accompanied by the disadvantage of low signal-noise ratio of EIT spectrum. The possible solution of increasing signal-to-noise ratio is using the Mach–Zehnder interferometer detection[24] or a frequency modulation technique.[25] In future work, the squeezed probe beam will be used to decrease the shot noise and to improve the Rydberg-atom-based field measurements.

References

[1] Heavner T P, Donley E A, Levi F, Costanzo G, Parker T E, Shirley J H, Ashby N, Barlow S and Jefferts S R 2014 *Metrologia* **51** 174
[2] Ludlow A D, Boyd M M, Ye Jun, Peik E and Schmidt P O 2015 *Rev. Mod. Phys.* **87** 637
[3] Savukov I M, Seltzer S J, Romalis M V and Sauer K L 2005 *Phys. Rev. Lett.* **95** 063004
[4] Patton B, Versolato O O, Hovde D C, Corsini E, Higbie J M and Budker D 2012 *Appl. Phys. Lett.* **101** 083502

[5] Gallagher T F 1994 *Rydberg Atoms* (Cambridge: Cambridge University Press)

[6] Holloway C L, Gordon J A, Jefferts S, Schwarzkopf A, Anderson D A, Miller S A, Thaicharoen N and Raithel G 2014 *IEEE Trans. Antennas Propag.* **62** 6169

[7] Sedlacek J A, Schwettmann A, Kübler H, Löw R, Pfau T and Shaffer J P 2012 *Nat. Phys.* **8** 819

[8] Fan H, Kumar S, Sedlacek J, Kübler H, Karimkashi S and Shaffer J P 2015 *J. Phys. B: At. Mol. Opt. Phys.* **48** 202001

[9] Holloway C L, Simons M T, Gordon J A, Dienstfrey A, Anderson D A and Raithel G 2017 *J. Appl. phys.* **121** 233106

[10] Zhang L J, Liu J S, Jia Y, Zhang H, Song Z F and Jia S T 2018 *Chin. Phys. B* **27** 033201

[11] Gordon J A, Holloway C L, Schwarzkopf A, Anderson D A, Miller S, Thaicharoen N and Raithel G 2014 *Appl. Phys. Lett.* **105** 024104

[12] Jiao Y C, Han X X, Yang Z W, Li J K, Raithel G, Zhao J M and Jia S T 2016 *Phys. Rev. A* **94** 023832

[13] Jiao Y C, hao L P, Han X X, Bai S Y, Raithel G, Zhao J M and Jia S T 2017 *Phys. Rev. Appl.* **8** 014028

[14] Jiao Y C, Zhao J M and Jia S T 2018 *Acta Phys. Sin.* **67** 073201 (in Chinese)

[15] Fleischhauer M, Imamoglu A and Marangos J P 2005 *Rev. Mod. Phys.* **77** 633

[16] Mohapatra A K, Jackson T R and Adams C S 2007 *Phys. Rev. Lett.* **98** 113003

[17] Fan H Q, Kumar S, Daschner R, Kübler H and Shaffer J P 2014 *Opt. Lett.* **39** 3030

[18] Holloway C L, Gordon J A, Schwarzkopf A, Anderson D A, Miller S A, Thaicharoen N and Raithel G 2014 *Appl. Phys. Lett.* **104** 244102

[19] Fan H Q, Kumar S, Sheng J, Shaffer J P, Holloway C L and Gordon J A 2015 *Phys. Rev. Appl.* **4** 044015

[20] Yan L Y, Liu J S, Zhang H, Zhang L J, Xiao L T and Jia S T 2017 *Acta Phys. Sin.* **66** 243201 (in Chinese)

[21] Autler S H and Townes C H 1955 *Phys. Rev.* **100** 703

[22] Fan J B, Jiao Y C, Hao L P, Xue Y M, Zhao J M and Jia S T 2018 *Acta Phys. Sin.* **67** 093201 (in Chinese)

[23] Hao L P, Jiao Y C, Xue Y M, Han X X, Bai S Y, Zhao J M and Raithel G 2018 *New J. Phys.* **20** 073024

[24] Kumar S, Fan H Q, Kübler H, Sheng J T and Shaffer J P 2017 *Sci. Rep.* **7** 42981

[25] Kumar S, Fan H Q, Kübler H, Jahangiri A J and Shaffer J P 2017 *Opt. Exp.* **25** 8625